EUROfusion

EUROFUSION CP(15)06/34

N. Lemahieu et al.

H/He Irradiation on Tungsten Exposed to ELM-Like Thermal Shocks

12th International Symposium on Fusion Nuclear Technology (ISFNT)
Jeju Island, Korea
(14th September 2015 – 18th September 2015)

This work has been carried out within the framework of the EUROfusion Consortium and has received funding from the Euratom research and training programme 2014-2018 under grant agreement No 633053. The views and opinions expressed herein do not necessarily reflect those of the European Commission.

H/He irradiation on tungsten exposed to ELM-like thermal shocks

Nathan Lemahieu[a,c,d,1,*], Henri Greuner[b], Jochen Linke[a], Hans Maier[b], Gerald Pintsuk[a], Marius Wirtz[a], Guido Van Oost[c], Jean-Marie Noterdaeme[c,d]

[a] *Institute for Energy and Climate Research, Forschungszentrum Jülich, 52425 Jülich, Germany*
[b] *Max Planck Institute for Plasma Physics, 85748 Garching, Boltzmannstraße 2, Germany*
[c] *Department of Applied Physics, Ghent University, Sint-Pietersnieuwstraat 41 B4, 9000 Gent, Belgium*
[d] *Institute of Interfacial Process Engineering and Plasma Technology IGVP, Universität Stuttgart, Pfaffenwaldring 31, 70569 Stuttgart, Germany*

Abstract

ELM-like thermal shocks and H/He particle exposure were subsequently applied on tungsten samples. Polished test specimens underwent in the JUDITH 1 electron beam facility 100 transient thermal events with a duration of 1 ms. The absorbed heat flux was 0.4 GW m^{-2} and 1.5 GW m^{-2}, which is above the material's damage threshold. These experiments were done at room temperature and with the samples heated to 400 °C base temperature. Depending on the loading conditions the test specimens have either a crack network or showed surface roughening. The samples were then loaded in the GLADIS facility at different surface temperatures with a mixed H/He beam with a flux of 3.7×10^{21} m^{-2} s. Post-mortem analysis showed that the roughened surface did not alter the H/He induced surface modifications. In contrast to that on the test specimens that exhibited crack formation, phenomena such as bubble creation along the crack edge, formation of a shallow layer of nano-structures covering the crack opening, and the emerging of a porous structure which partially fills the crack are observed.

Keywords: ELMs, Tungsten, High Heat Flux tests, Surface morphology, Helium, Hydrogen

1. Introduction

Plasma facing materials (PFMs) will be exposed to a combination of various particle fluxes, heat loads and fast neutron irradiation in a fusion reactor. Tungsten has been selected as PFM in several fusion experiments due to advantageous material properties, such as its thermal conductivity, tritium retention, and erosion rate. Nevertheless, each of the occurring loading conditions can harm the tungsten armour to unacceptable levels. Since each exposure has a different damage mechanism, it is relevant not only to study each exposure condition separately, but also to understand the interplay between loading conditions.

Edge localized modes (ELMs) and steady state particle irradiation are two types of loading conditions that might damage tungsten. Roughening of the surface, formation of crack networks, and melting are examples of the damages induced by ELMs [1]. Particle exposure can lead to sub-surface bubble formation, blistering, and the appearance of He-induced nano-structures, so called *fuzz* [2]. However, the damage of these two exposures can influence each other and result in synergistic effects.

Several studies have been performed, in which these loading conditions have been applied on tungsten either simultaneously or after each other [3–6]. Both beneficial and disadvantageous effects have been identified in these experiments, but there are still focus-points missing to obtain a comprehensive understanding of the synergistic effects. Therefore, the influence of ELM-like pre-exposed surfaces on the damage behaviour of particle exposure is specifically investigated in this work, through successive ELM-like loading conditions and H/He-irradiation.

2. Material and Methods

A double forged tungsten disk, produced by Plansee, was used to obtain the test specimens. The sample shapes are blocks with a length of 10 mm, a width of 5 mm, and a varying height between 5 mm and 15 mm. The material's anisotropic microstructure has elongated grains parallel to the sample surface. This material was already previously characterized [7] and used in experiments with combined loading conditions [3].

JUDITH 1, a high heat flux facility at Forschungszentrum Jülich [8], was used to simulate the transient heat load of ELMs. Each sample was exposed to 100 thermal shocks applied by a 120 keV electron beam. The focussed beam has a diameter of 1 mm and scans for 1 ms the polished sample surface on a square of 16 mm^2. Experiments were done with an absorbed power density of 0.4 GW m^{-2} or 1.5 GW m^{-2}. Furthermore, the test specimens were either heated to a base temperature of 400 °C or kept at

*Corresponding author
Email address: n.lemahieu@fz-juelich.de (Nathan Lemahieu)
[1] Postal adress: Forschungszentrum Jülich, Nathan Lemahieu, IEK-2, 52425 Jülich, Germany, tel.: +49 2461 61-6300

room temperature (RT). These experiments are focussed on the heat loads of ELMs and do not take into account the particle flux associated with ELMs or the simultaneous steady state loading.

After the ELM-like loading conditions, mock-ups, similar to the ones used in earlier experiments [3], are produced by brazing samples to an active cooling structure. These mock-ups are exposed in the neutral beam facility GLADIS, located at the Max-Planck-Institut für Plasmaphysik Garching [9]. The beam has a Gaussian profile consisting out of a H/He mix with 6 at% He. It is generated from an ion source at 29 kV acceleration voltage and has a pulse duration of 30 s. This means that the particle energy is higher than expected for steady-state tokamak operation. At the beam centre, the particle flux is $3.7 \times 10^{21}\,\mathrm{m}^{-2}\,\mathrm{s}$, resulting in a heat flux of $10.5\,\mathrm{MW\,m}^{-2}$. The total particle fluence at the centre of the beam is $2 \times 10^{25}\,\mathrm{m}^{-2}$ after the exposure, which consists out of 180 pulses. Depending on both the sample height and the location with respect to the beam centre, the surface temperature during exposure is either 1500 °C, 1000 °C, or 600 °C.

Test specimens with all four JUDITH 1 pre-exposures were tested in GLADIS at a surface temperature of 1000 °C and 600 °C. GLADIS-exposure at a surface temperature of 1500 °C was only performed on samples with a JUDITH 1 pre-exposure of $0.4\,\mathrm{GW\,m}^{-2}$ at RT, $0.4\,\mathrm{GW\,m}^{-2}$ at 400 °C, and $1.5\,\mathrm{GW\,m}^{-2}$ at 400 °C.

After the combined exposures, the samples were analysed through laser profilometry, light microscopy, scanning electron microscopy (SEM) and focussed ion beam (FIB). In addition, analyses were performed on polished samples that only underwent the JUDITH 1 loading conditions as reference. For comparison reasons, also data from previous experiments [3] are used as a reference for the GLADIS exposure.

3. Results and Discussion

The JUDITH 1 exposure damaged the samples for each loading condition, which was expected since the lowest tested heat flux, $0.4\,\mathrm{GW\,m}^{-2}$, is above the material's damage threshold [7]. On each sample, the loaded area and the thermal shock induced damage can already be seen by visual inspection. Samples with exposures at a 400 °C base temperature only exhibited surface roughening. The severity of this roughening was highest for the maximum power density.

For the thermal shocks at room temperature, a crack network is formed throughout the exposed area, independent of the power density. At some crack edges of the $1.5\,\mathrm{GW\,m}^{-2}$ loaded samples, traces of local melting can be observed, as shown in figure 1. This is explained by a locally reduced heat transport capability between the surface and the bulk material, depending on the crack characteristics.

Both the surface morphology and the near-surface layer is modified after GLADIS exposure due to erosion and particle implantation. Different structures can be found on the top of the samples that had a surface temperature of 1500 °C or 1000 °C. As shown in figure 2, these extrusions also vary with the grain orientation. The samples with a 600 °C surface temperature, did not have such structures and can be characterized by an erosion pattern with height differences and holes on the surface.

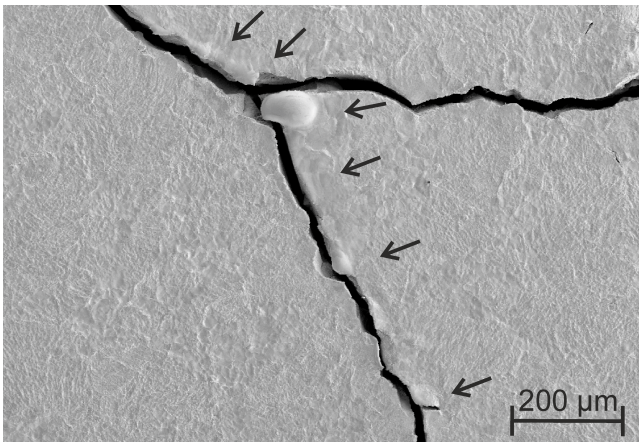

Figure 1: SEM image of tungsten after 100 ELM-like thermal shocks of $1.5\,\mathrm{GW\,m}^{-2}$ at RT, showing a part of the formed crack network with a tungsten droplet and indications of other local melting events at the edges of the crack.

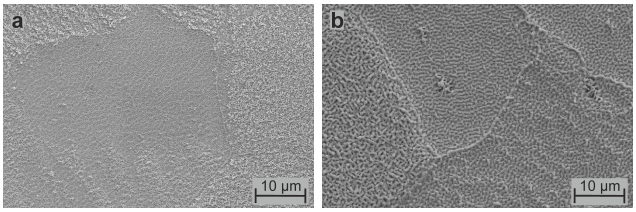

Figure 2: SEM images of polished tungsten exposed to an H/He-beam in GLADIS with a surface temperature of 1000 °C (a) and 1500 °C (b).

While the reference samples were polished to a mirror-like finish before the particle exposure, the erosion and surface extrusions altered the optical reflectivity. Due to these effects the surface colour changed to grey, black, and matt after loading at a surface temperature of 1500 °C, 1000 °C, and 600 °C respectively. In addition, recrystallization occurred for the experiments at 1500 °C.

After the combined exposures, the surface from those samples exposed to the H/He-beam at 1500 °C looks homogeneously in a visual inspection. The loaded area from the thermal shock experiments are is longer detectable without optical equipment. The whole surface is covered with extrusions that are all similar, independent of the ELM-like pre-exposure on the sample. The apparent minor differences between the extrusions in figure 3, are considered to be coming from the tilt angle of the SEM-pictures and the crystal orientation of the grain on which the extrusions have grown.

In the case of the sample that exhibited a crack net-

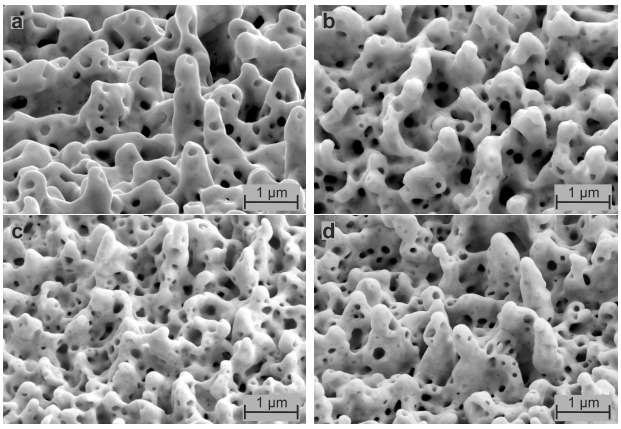

Figure 3: SEM pictures with different tilting angles from tungsten exposed to H/He-flux at 1500 °C surface temperature, for a reference sample without pre-exposure (a), with ELM-like thermal shock pre-exposure of 0.4 GW m^{-2} at RT (b), with ELM-like thermal shock pre-exposure of 0.4 GW m^{-2} at 400 °C (c), and with ELM-like thermal shock pre-exposure of 1.5 GW m^{-2} at 400 °C (d), showing the surface extrusions.

work after thermal shock testing, the cracks are still clearly visible in the SEM pictures. As depicted in figure 4, the sample exhibited *crack bridging*, when the surface structures have grown in a way that it locally covers (partially) the crack. Since this is observed on several but not on all crack locations, only certain circumstances lead to the occurrence of this phenomena. It is suggested that potential factors prohibiting crack bridging could be the incidence angle of the particle flux, the grain orientation, a large crack width, and the direction in which the crack propagates on the sample surface. FIB-cuts on these *bridge*-features, show that this is a shallow material layer of surface structures that connect the crack edges and does not provide an adequate crack-repair in the depth. These FIB-cuts show also that sub-surface bubbles are generated along the crack edges. Furthermore, on certain locations inside the sample, the crack locally reconnected. Through comparing a series of FIB-cuts on the same crack, it is concluded that this could happen due to the grain growth during the recrystallization.

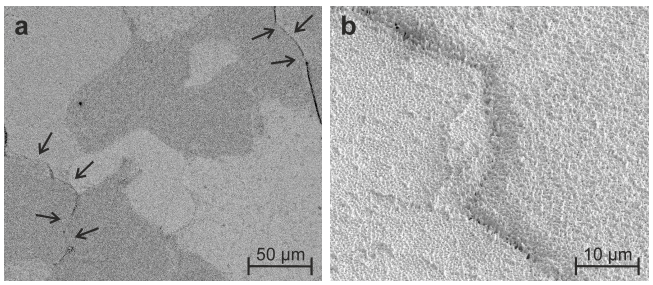

Figure 4: Examples of the *crack bridging* effect for a tungsten sample first exposed to 0.4 GW m^{-2} thermal shocks at RT and subsequently irradiated by a H/He particle flux with a surface temperature of 1500 °C.

Also for the test specimens, which had a surface temperature of 1000 °C during particle exposure, the area first loaded in JUDITH 1 is not detectable without any optical equipment. As happened with the reference sample, the surfaces of the pre-exposed samples are black after GLADIS exposure. The only exception is for the sample with 1.5 GW m^{-2} thermal shock pre-exposure at RT, where the whole surface is also black, but the loaded area is still visible, albeit barely. It is worth noting that this particular pre-exposure was not part of the experiments with the 1500 °C surface temperature samples.

For each of the four 1000 °C test specimens, the extrusion growth has not been noticeably modified due to the ELM-like pre-exposure. Nevertheless, these surface structures, shown in figure 5, do not look completely identical. This is again an effect from the crystal orientation and the different tilt angles in the SEM-pictures. This similarity also holds, when these four samples are compared with the earlier published figure from the reference sample [3].

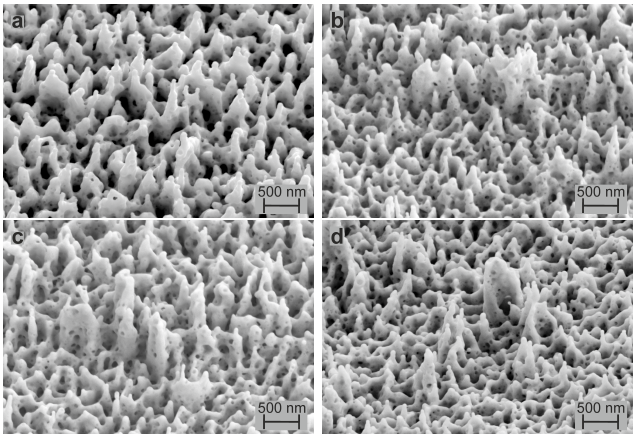

Figure 5: The surface extrusions of tungsten loaded with an H/He-beam at 1000 °C for test specimens with various pre-exposures. 0.4 GW m^{-2} thermal shocks at RT (a), 0.4 GW m^{-2} thermal shocks at 400 °C (b), 1.5 GW m^{-2} thermal shocks at RT (c), and 1.5 GW m^{-2} thermal shocks at 400 °C (d). The tilt angle is not identical for each SEM-image.

The two cracked 1000 °C samples are also examined for particle effects at the crack. SEM investigation shows that, as long as the crack edge is not too steep, the surface structures also grow on the crack edge. As figure 6 shows, also the *crack bridging* features are present for both test specimens. Although no comparative study is done due to a lack of a sufficiently high amount of *bridging* effects, this seems to occur more sparsely for these 1000 °C samples, than for the earlier discussed 1500 °C samples.

In addition, the bubble growth at the crack edges have now created a porous sponge-like filling in a part of the crack, as is shown by the FIB-section in figure 7. The cavities in this *sponge structure* are larger than the surface extrusions. Several FIB-cuts with an distance of 50 nm between them are taken of the same crack, from which it follows that the cavities are interconnected with each other.

The samples exposed to the H/He-beam at a surface

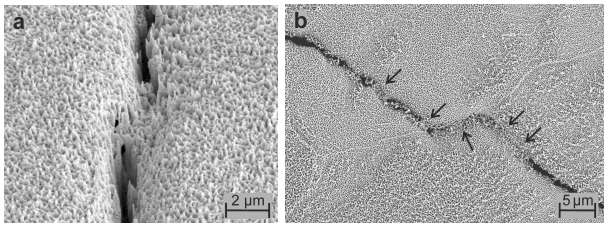

Figure 6: *Crack bridging* for tungsten first exposed to thermal shocks at RT with a power density of 0.4 GW m^{-2} (a) and 1.5 GW m^{-2} (b), and then irradiated with a H/He-beam at 1000 °C.

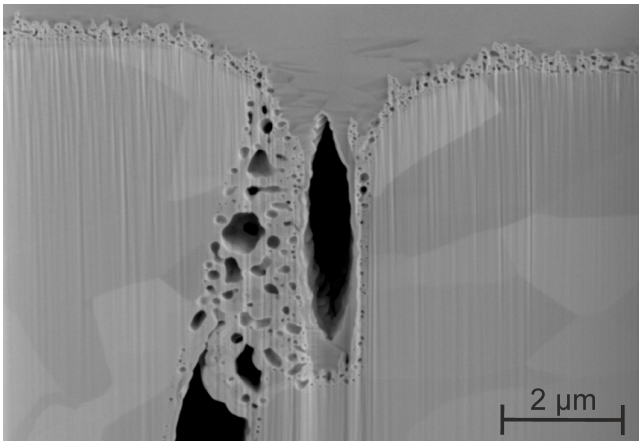

Figure 7: FIB-section showing a porous structure partially filling a crack for tungsten exposed to a H/He flux at 1000 °C, after it first underwent 0.4 GW m^{-2} thermal shocks at RT.

temperature of 600 °C have a matt surface, just like the reference sample. In a visual inspection only the JUDITH 1 exposed area at RT with 0.4 GW m^{-2} thermal shocks can not be detected without optical equipment. The erosion patterns on all four specimens are the same as on the reference sample. No special features, such as *crack bridging*, are found in neither SEM pictures or FIB-sections.

For the cracked samples, the mechanism behind the He-induced sub-surface cavities and surface extrusions play a vital role in the material behaviour. Recrystallization is apparently not a necessary condition, since also the 1000 °C samples exhibited phenomena like *crack bridging*, formation of a porous structure, and bubble generation at the crack edge. Due to the fact that these features can act as thermal barrier in the material, this could become problematic. When this results in local overheating of the surface, melting can occur for lower heat loads than expected. In addition, the thermo-mechanical stability of such porous crack filling structures and *crack bridges* are not yet analysed. Both phenomena might act as an unanticipated source of tungsten dust by material erosion, which could increase the speed of deterioration for tungsten as a PFM. It is therefore necessary to conduct further experiments, so the consequences can be determined.

Due to the high energy of the H/He-beam, the erosion on each sample should be at least 1.0 µm due to physical sputtering, although experimental data showed higher erosion [10]. To determine quantitatively if the erosion affected the ELM-induced damage, the surface roughness was measured. With laser profilometry the samples are scanned with both a 250 points/mm and a 50 points/mm surface scan. This lateral resolution is not accurate enough to be sensitive for the surface structures induced by the H/He-beam. From the profilometry data the arithmetic mean roughness R_a of the exposed area is determined according to the ISO 4287/1 standard. For a given sample, the difference between the two data sets is lower than 0.1 µm. The calculated R_a, sorted by the ELM-like pre-exposure in JUDITH 1, is depicted in figure 8.

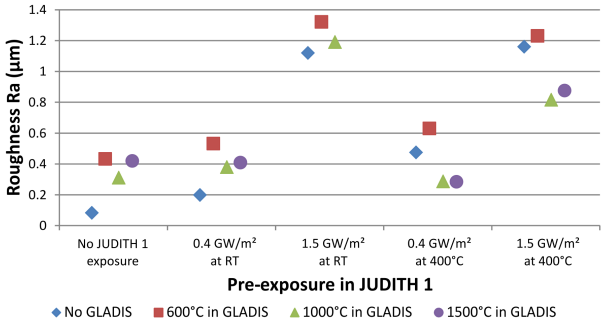

Figure 8: The arithmetic mean roughness R_a calculated from a 50 points/mm laser profilometry scan.

Naturally, the unexposed polished sample, which is indicated with 'no GLADIS - no JUDITH 1', has a lower roughness than the GLADIS-reference samples. Also for the JUDITH 1 exposure with the lowest loading condition, 0.4 GW m^{-2} at RT, this is still the case, although the differences in R_a are smaller. This is related to the R_a being mainly determined by the cracks, since the inter-crack surface is smooth with this particular pre-exposure. Only for the samples that only roughened during the thermal shocks, i.e. the 400 °C ELM-like loads, and were subsequently exposed in GLADIS at 1500 °C or 1000 °C, there is a modest roughening decrease. This is considered to come from erosion, since the method is not sensitive to the surface structures. Nevertheless, all samples still show the same trend, which is visible when the data-points for the same GLADIS-exposure would be connected.

In these experiments, the energy of the incident H and He particles in GLADIS is higher than expected for divertor conditions, resulting in an increased erosion-rate. The occurrence of ELMs would also be higher, since they would happen with a frequency of several Hz. Therefore, the modification caused by erosion of the ELM-induced roughness should be reduced. This might suggest that the erosion would only have a minimal effect on the cumulative ELM-roughening, since this ELM-damage would occur faster than the erosion might alter it.

4. Conclusions

The damage of H/He-irradiation was investigated for tungsten samples that were priorly exposed to ELM-like thermal loads. Depending on the type of ELM-induced damage, different conclusions are made.

Roughened test specimens, i.e. loaded at a 400 °C base temperature in JUDITH 1, did not result in an altered H/He damage behaviour. The erosion patterns and/or surface extrusion that emerged after the particle exposure are for each surface temperature in GLADIS, similar to each other and to the GLADIS-reference sample. For the 1500 °C and 1000 °C samples, the erosion did result in a reduced roughness. However, this is not considered to change the cumulative ELM-induced roughening, due to the different time-scales in which ELMs and erosion occur in a tokamak environment.

Cracked test specimens, i.e. loaded at a RT base temperature in JUDITH 1, also had unchanged erosion patterns and/or surface extrusions. Also the erosion did not decrease the roughness that originated from the ELM-like thermal shocks. But the particle exposure did strongly influence the cracks, if surface extrusions were created. This includes the formation of surface structures within the crack, the *bridging* of the crack opening, bubble formation along the crack surface, and an porous *sponge*-like structure that emerged in the crack. The consequences of these features are not clear, but might include overheating, melting, and increased dust production. Therefore, further dedicated research is necessary to determine the significance of these phenomena.

Acknowledgements

The authors gratefully acknowledge M. Balden, S. Elgetti, D. Eßer, D. Grüner, and E. Wessel for the SEM and FIB images.

This work was supported by the European Commission and carried out within the framework of the Erasmus Mundus International Doctoral College in Fusion Science and Engineering (FUSION-DC). This work was executed under EUROfusion WP PFC. This work has been carried out within the framework of the EUROfusion Consortium and has received funding from the Euratom research and training programme 2014-2018 under grant agreement No 633053. The views and opinions expressed herein do not necessarily reflect those of the European Commission.

References

[1] K. Wittlich, T. Hirai, J. Compan, N. Klimov, J. Linke, A. Loarte, M. Merola, G. Pintsuk, V. Podkovyrov, L. Singheiser, A. Zhitlukhin, Damage structure in divertor armor materials exposed to multiple ITER relevant ELM loads, Fusion Engineering and Design 84 (711) (2009) 1982–1986. doi:10.1016/j.fusengdes.2008.11.049.

[2] J. Ueda, J. W. Coenen, G. De Temmerman, R. P. Doerner, J. Linke, V. Philipps, E. Tsitrone, Research status and issues of tungsten plasma facing materials for ITER and beyond, Fusion Engineering and Design 89 (2014) 901–906. doi:10.1016/j.fusengdes.2014.02.078.

[3] N. Lemahieu, H. Greuner, J. Linke, H. Maier, G. Pintsuk, G. Van Oost, M. Wirtz, Synergistic effects of ELMs and steady state H and H/He irradiation on tungsten, Fusion Engineering and Design ? (2015) In Press. doi:10.1016/j.fusengdes.2015.06.051.

[4] D. Nishijima, R. P. Doerner, D. Iwamoto, Y. Kikuchi, M. Miyamoto, M. Nagata, I. Sakuma, K. Shoda, Y. Ueda, Response of fuzzy tungsten surfaces to pulsed plasma bombardment, Journal of Nuclear Materials 434 (1-3) (2013) 230–234. doi:10.1016/j.jnucmat.2012.10.042.

[5] G. De Temmerman, J. Zielinski, S. van Diepen, L. Marot, M. Price, Elm simulation experiments on pilot-psi using simultaneous high flux plasma and transient heat/particle source, Nuclear Fusion 51 (2011) 073008. doi:10.1088/0029-5515/51/7/073008.

[6] M. Wirtz, J. Linke, G. Pintsuk, G. De Temmerman, G. M. Wright, Thermal shock behaviour of tungsten after high flux H-plasma loading, Journal of Nuclear Materials 443 (1-3) (2013) 497–501. doi:10.1016/j.jnucmat.2013.08.002.

[7] G. Pintsuk, A. Prokhodtseva, I. Uytdenhouwen, Thermal shock characterization of tungsten deformed in two orthogonal directions, Journal of Nuclear Materials 417 (2011) 481–486. doi:10.1016/j.jnucmat.2010.12.109.

[8] R. Duwe, W. Kühnlein, H. Münstermann, The new electron beam facility for materials testing in hot cells - design and preliminary experience, Fusion Technology (1994) 355–358doi:10.1016/B978-0-444-82220-8.50057-1.

[9] H. Greuner, B. Boeswirth, J. Boscary, P. McNeely, High heat flux facility GLADIS: Operational characteristics and results of W7-X pre-series target tests, Journal of Nuclear Materials 367–370 (2007) 1444–1448. doi:10.1016/j.jnucmat.2007.04.004.

[10] H. Maier, H. Greuner, M. Balden, B. Böswirth, S. Lindig, C. Linsmeier, Erosion behavior of actively cooled tungsten under H/He high heat flux load, Journal of Nuclear Materials 438 (2013) S921–S924. doi:10.1016/j.jnucmat.2013.01.200.